Cardiology in the Young

cambridge.org/cty

Expert Consensus Statement: Anatomy, Imaging, and Nomenclature of Congenital Aortic Root Malformations

Justin T. Tretter MD[1], Diane E. Spicer BS, PA(ASCP)[2,3], Rodney C. G. Franklin MD[4], Marie J. Béland MD[5], Vera D. Aiello MD, PhD[6], Andrew C. Cook PhD[7], Adrian Crucean MD, PhD[8], Rohit S. Loomba MD[9], Shi-Joon Yoo MD, PhD[10], James A. Quintessenza MD[2], Christo I. Tchervenkov MD[11], Jeffrey P. Jacobs MD[3], Hani K. Najm MD[12] and Robert H. Anderson MD, PhD[13]

[1]Department of Pediatric Cardiology, Cleveland Clinic Children's and The Heart, Vascular, and Thoracic Institute, Cleveland Clinic, Cleveland, Ohio; [2]Heart Institute, Johns Hopkins All Children's Hospital, St Petersburg, Florida; [3]Congenital Heart Center, UF Health Shands Hospital, Division of Cardiovascular Surgery, Departments of Surgery and Pediatrics, University of Florida, Gainesville, Florida; [4]Paediatric Cardiology Department, Royal Brompton & Harefield National Health Service Trust, London, United Kingdom; [5]Division of Pediatric Cardiology, The Montreal Children's Hospital of the McGill University Health Centre, Montréal, Québec, Canada; [6]Heart Institute (InCor), University of São Paulo School of Medicine, São Paulo, Brazil; [7]Institute of Cardiovascular Science, University College London, London, United Kingdom; [8]Department of Paediatric Cardiac Surgery, Birmingham Women's and Children's Hospital, Birmingham, United Kingdom; [9]Division of Cardiology, Advocate Children's Hospital, Oak Lawn, Illinois; [10]Division of Cardiology, Department of Pediatrics, Labatt Family Heart Centre, Hospital for Sick Children, University of Toronto, Toronto, Ontario, Canada; [11]Division of Cardiovascular Surgery, The Montreal Children's Hospital of the McGill University Health Centre, Montréal, Québec, Canada; [12]Division of Pediatric Cardiac Surgery, Cleveland Clinic Children's and the Heart, Vascular, and Thoracic Institute, Cleveland Clinic, Cleveland, Ohio and [13]Cardiovascular Research Centre, Biosciences Institute, Newcastle University, Newcastle upon Tyne, United Kingdom

Abstract

Over the past 2 decades, several categorizations have been proposed for the abnormalities of the aortic root. These schemes have mostly been devoid of input from specialists of congenital cardiac disease. The aim of this review is to provide a classification, from the perspective of these specialists, based on an understanding of normal and abnormal morphogenesis and anatomy, with emphasis placed on the features of clinical and surgical relevance. We contend that the description of the congenitally malformed aortic root is simplified when approached in a fashion that recognizes the normal root to be made up of 3 leaflets, supported by their own sinuses, with the sinuses themselves separated by the interleaflet triangles. The malformed root, usually found in the setting of 3 sinuses, can also be found with 2 sinuses, and very rarely with 4 sinuses. This permits description of trisinuate, bisinuate, and quadrisinuate variants, respectively. This feature then provides the basis for classification of the anatomical and functional number of leaflets present. By offering standardized terms and definitions, we submit that our classification will be suitable for those working in all cardiac specialties, whether pediatric or adult. It is of equal value in the settings of acquired or congenital cardiac disease. Our recommendations will serve to amend and/or add to the existing International Paediatric and Congenital Cardiac Code, along with the Eleventh iteration of the International Classification of Diseases provided by the World Health Organization.

Original Article

Cite this article: Tretter JT, Spicer DE, Franklin RCG, Béland MJ, Aiello VD, Cook AC, Crucean A, Loomba RS, Yoo S-J, Quintessenza JA, Tchervenkov CI, Jacobs JP, Najm HK, and Anderson RH (2023) Expert Consensus Statement: Anatomy, Imaging, and Nomenclature of Congenital Aortic Root Malformations. *Cardiology in the Young* **33**: 1060–1068. doi: 10.1017/S1047951123001233

Received: 3 May 2023
Accepted: 4 May 2023
First published online: 8 June 2023

Corresponding author: Dr Tretter, Pediatric and Adult Congenital Heart Center, Cleveland Clinic, 9500 Euclid Ave, M-41, Cleveland, OH 44195; email: trettej3@ccf.org.

Accepted for publication Mar 15, 2023.

This article has been co-published in *The Annals of Thoracic Surgery* and *Cardiology in the Young*.

The Society of Thoracic Surgeons requests that this article be cited as: Tretter JT, Spicer DE, Franklin RCG, et al. Expert Consensus Statement: Anatomy, Imaging, and Nomenclature of Congenital Aortic Root Malformations. *Ann Thorac Surg*. 2023; in press.

The Supplemental Tables, Figures, and Videos can be viewed in the online version of this article [https://doi.org/10.1016/j.athoracsur.2023.03.023] on https://www.annalsthoracicsurgery.org.

Over the last 15 years, several schemes have been proposed for categorization of abnormalities of the aortic root, particularly the so-called bicuspid aortic valve and its associated aortopathies.[1–4] Most have been written by specialists treating adult patients with otherwise normal hearts. These fall short when seeking to correlate the relevant 3-dimensional complexity of the aortic root with accurate and logical classification schemes capable of accounting for the entire

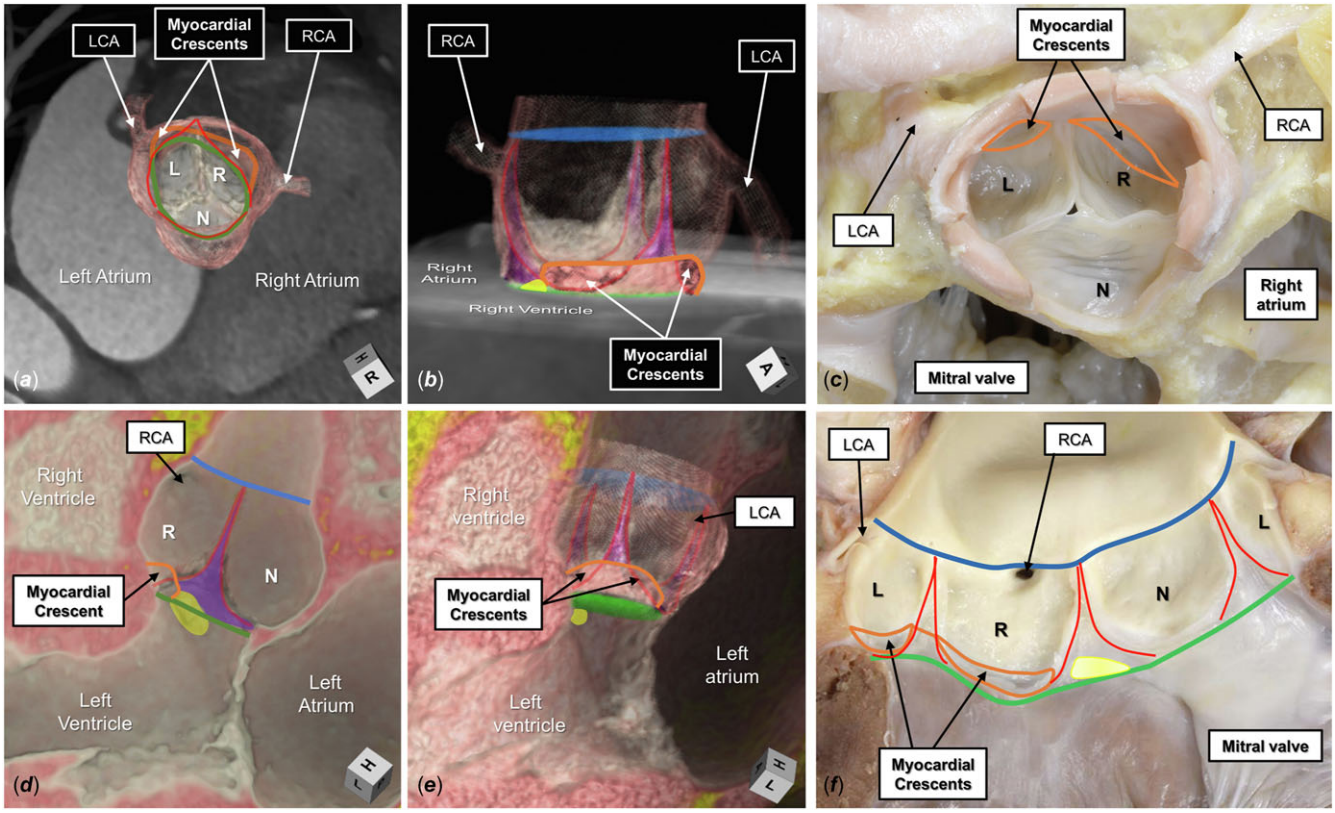

Figure 1. The normal aortic root is shown by 3-dimensional computed tomographic reconstruction in its (A) short axis and (B) long axis, viewing the myocardial-arterial junction incorporated between the coronary sinuses (orange line). The semilunar lines of attachment, in red, extend from the sinutubular junction, colored blue, to the level of the virtual basal ring, colored green. The interleaflet triangles are colored purple. In panel B, the superior aspect of the membranous septum is colored yellow and merges with the base of the interleaflet triangle separating the right (R) and noncoronary (N) aortic sinuses. (C) A comparable autopsied heart specimen. (D) A virtual dissection of a long-axis plane of the root. (E) The entirety of the root is added. (F) The comparable autopsied heart. (L, left coronary aortic sinus; LCA, left coronary artery; RCA, right coronary artery.)

spectrum encountered when the root is congenitally malformed.[1–3] We offer here a perspective from the stance of specialists in congenital cardiac disease. We based our approach on an understanding of normal and abnormal morphogenesis and anatomy, with emphasis placed on the features of clinical and surgical relevance. We anticipate that our suggested terms and definitions will be of value across all cardiac specialties, whether pediatric or adult, and will prove of equal value in describing acquired and congenital cardiac disease.

Anatomy of the normal aortic root

The aortic root is a complex, 3-dimensional, structure extending proximally from the virtual basal ring to the sinutubular junction distally, made up of 3 individual leaflets, each attached within their supporting sinus in semilunar fashion, with the sinuses separated by the interleaflet triangles (Supplemental Table 1).[5] Each leaflet is attached distally at the sinutubular junction, and its nadir is at the level of the virtual basal ring (Figure 1). The overall arrangement produces a crown-like configuration.

During diastole, 3 peaks of the crown, usually named as commissures, can be identified at the attachments of the leaflets at the sinutubular junction. The zones of apposition between the leaflets then extend radially from the commissures to the centroid of the valvar orifice.[6] The space proximal to the skirt of tissue provided by the leaflets during diastole, which is distal to the plane of the virtual basal ring, hemodynamically is part of the left ventricular outflow tract.[6,7]

The surface areas of coaptation span between the centrally positioned nodules of Arantius and the peripherally positioned commissures. The areas of apposition on either side of these nodules are known as the lunules, with the greatest surface area of coaptation found midway within each lunule.[4,8] Noncoapting areas, the bellies, extend to the margins of the semilunar hinges and serve as the interface of the hemodynamic ventriculoarterial junction in diastole. The commissures form the apexes of the interleaflet triangles, with the triangles themselves forming the walls of the root belonging to the left ventricular outflow tract (Figure 2).

The virtual basal ring, or echocardiographic "annulus," is the geometric planar surface, limited by the confines of the aortic root, created by joining the nadirs of attachment of the leaflets. It marks the proximal anatomical boundary of the aortic root. The sinutubular junction forms the distal boundary between the root and the ascending aorta (Figures 1, 2).[6]

The virtual basal ring should not be equated with the ventriculoarterial junction. This latter junction, better described as being myocardial-arterial, is usually found only in the sinuses giving rise to the coronary arteries and their intervening interleaflet triangle. It is crossed by the semilunar line of the attachment of the leaflets, with marked individual variation. The walls of the noncoronary aortic sinus, in contrast, lack myocardial support. This sinus is supported by the central fibrous body, and the fibrous curtain with the

https://doi.org/10.1017/S1047951123001233 Published online by Cambridge University Press

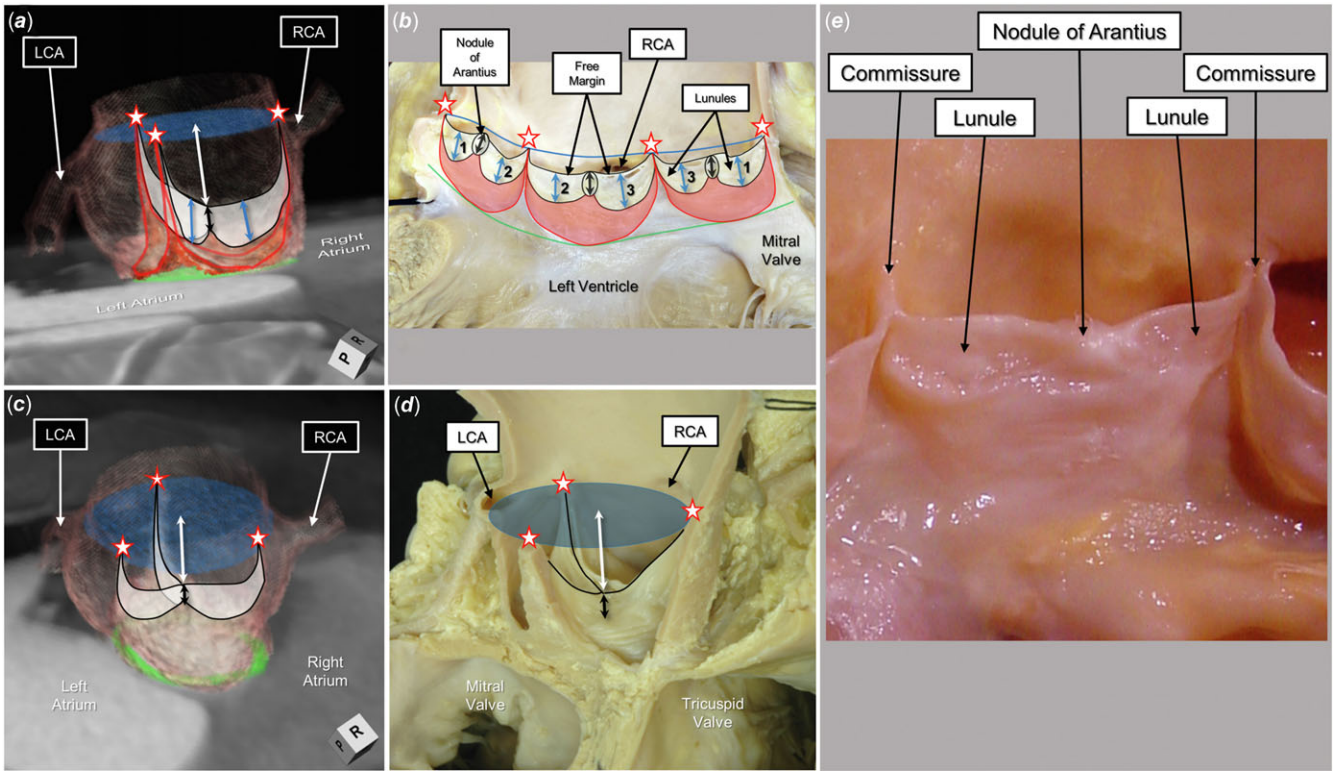

Figure 2. (A, C) Three-dimensional computed tomographic reconstructions of a normal aortic root during diastole. The 3 zones of apposition are colored white with black borders, comprising the components of the leaflets marked in panel E. The midpoint of coaptation is positioned just over halfway between the sinutubular junction, colored blue, and midportion of the root (white double-headed arrow), closer to the virtual basal ring, colored green. The zone of apposition increases in its midportion (blue double-headed arrows), before decreasing towards the commissures (white stars with red borders). The hemodynamic ventriculoarterial junction, formed by the leaflet bellies, is colored red, bordered peripherally by their semilunar attachments (red lines). This junction has 3 points peripherally at the commissures and a fourth shorter, central peak. The height of this central peak represents the difference between the effective height of the leaflets vs the coaptation length, the latter marked with a black double-headed arrow. (B, D) Comparable anatomy in an autopsied heart specimen. The lunules of adjacent coapting leaflets are labeled with corresponding numbers. (E) Components of the leaflets. (LCA, left coronary artery; RCA, right coronary artery.)

aortic leaflets of the mitral valve (Figure 1).[9,10] This fibrous curtain, spanning between the left and right fibrous trigones, also supports a variable portion of the left coronary leaflet.[11,12] The arrangement in the aortic root contrasts with the situation found in the pulmonary root, in which ventricular myocardium is incorporated into the bases of all 3 of its sinuses.[4,6]

When discussing the components of the roots, we have purposely avoided using the word "cusp." This word is currently used to account for either the leaflets or the sinuses, or a combination of both.[13,14] If used, we suggest this should be confined to a description of the leaflets. The interleaflet triangles are the fibrous walls of the root beneath the 3 peaks of the valvar crown.[15] The triangle between the right and noncoronary aortic sinuses is in continuity proximally with the membranous septum,[6,15–18] which is usually positioned such that part is distal to the virtual basal ring.[12,19] In most individuals, it is divided on the right side into atrioventricular and interventricular components by the attachment of the septal leaflet of the tricuspid valve.[11] In the setting of the normal trisinuate aortic root, it is almost always accurate to describe left and right coronary aortic sinuses. Should the coronary arterial origin be anomalous, these sinuses are better described as facing, or adjacent to, the pulmonary root. This permits a logical description should a coronary artery arise from the nonadjacent sinus.

The central fibrous body is an integral part of the ventricular support of the root.[19] Usually described as comprising the membranous septum and the right fibrous trigone,[20] it possesses a third part, namely, the roof of the inferoseptal recess of the left ventricular outflow tract. This area of fibrous continuity between the leaflets of the mitral and tricuspid valves supports the base of the buttress of the atrial septum. Its zone of continuity with the membranous septum is penetrated by the atrioventricular conduction axis.[21] The nonbranching bundle, positioned on the crest of the muscular septum, then courses along the inferior margin of the membranous septum, where it gives rise to the right and left bundle branches. The superior fascicle of the left bundle often ascends the crest of the muscular ventricular septum toward the nadir of the right coronary leaflet before slowly descending and wrapping around the left ventricular outflow tract toward the base of the superolateral papillary muscle.[19,21] It is appreciation of both the variability seen in the relationship of the inferior margin of the membranous septum relative to the plane of the virtual basal ring[12] and the common adjacency of the left bundle branch to the nadir of the right coronary leaflet that can guide the surgeon to avoid damage to the ventricular components of the conduction axis.[4,19,21]

Anatomy of the congenitally malformed aortic root

Description is greatly simplified when the components are assessed in terms of the number of sinuses present. Most frequently, the malformed root retains the trisinuate arrangement, although in a minority of cases it is bisinuate, or even more rarely, quadrisinuate (Figure 3; Supplemental Table 2).

https://doi.org/10.1017/S1047951123001233 Published online by Cambridge University Press

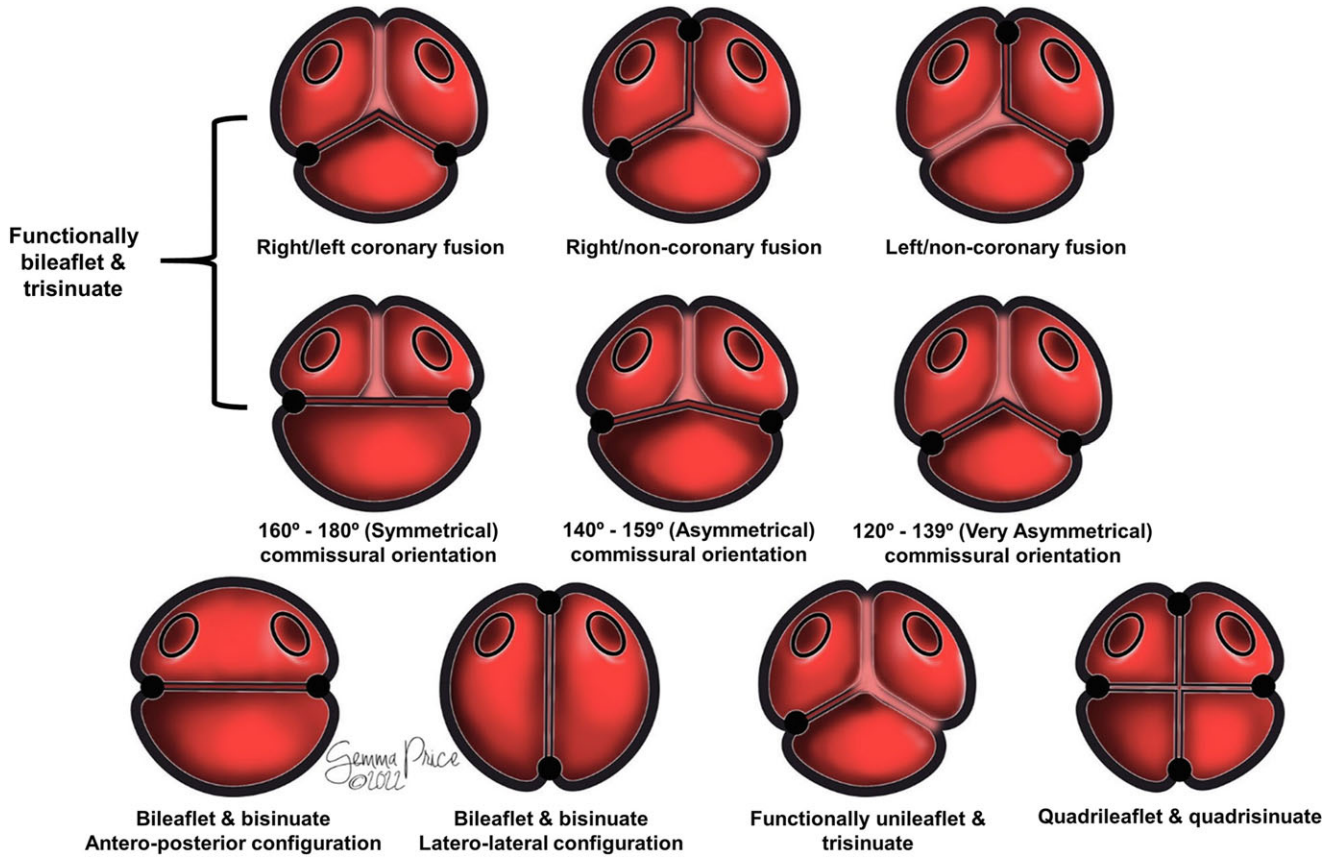

Figure 3. The drawing shows how classification of the congenitally malformed aortic root is simplified when described in terms of leaflets, sinuses, and interleaflet triangles.

Functionally bileaflet aortic valve

The functionally bileaflet, or "bicuspid," aortic valve is found in almost nine-tenths of all congenitally malformed roots.[22,23] Possessing 3 leaflets, sinuses, and interleaflet triangles, its presence reflects the fusion, during development, of 2 of the leaflets, with a resulting raphe. The corresponding interleaflet triangle is hypoplastic, no longer extending distally to reach the sinutubular junction. The "raphe" is the prominent tissue found at the site of fusion between the leaflets and can be variable in its extent. Fused variants have been described in its absence.[3] This could reflect ambiguity in the use of "raphe," or indicate that the lesions are bisinuate rather than trisinuate. We have yet, in our collective experiences, to encounter a trisinuate root with 2 functional leaflets lacking a raphe. When a zone of fusion is present, our evidence suggests that a raphe will be present, even if minimally formed. Should ambiguity persist, attention should be turned toward long-axis echocardiographic imaging and cross-sectional interrogation of the hypoplastic interleaflet triangle, which would be present in the trisinuate but not the bisinuate variant (Supplemental Figures 1, 2).

Incomplete fusion of less than half of the zone of apposition is commonly considered a "partial," or "forme fruste" bicuspid valve. We have found an inverse relationship between the length of the zone of fusion and the corresponding hypoplasia of the interleaflet triangle, with a spectrum from zero to complete (Figures 4A, 4B). This feature, along with asymmetry between the conjoined and third leaflets, dictates the plane of opening of the valvar orifice area relative to the long axis of the ascending aorta and to the plane of the sinutubular junction. Such asymmetry is pronounced compared with the normal aortic root.[6,22] The degree of asymmetry is held to guide the type of surgical repair, as well as predicting its durability.

In the so-called symmetrical arrangement, with the 2 commissures positioned directly opposite each other at 160° to 180°, the surgical recommendation is usually an approach which maintains its "bicuspid" form. When the commissures are at 120° to 139° from each other, the arrangement is said to be "very asymmetric," lending itself to "tricuspidization." The intermediate position is deemed "asymmetric" (Figure 3, middle row). Depending on the strategy used for repair, and the commissural orientation, repositioning of the commissures has been demonstrated to improve valvar function and durability.[24]

It is most usually the right and left coronary leaflets that are fused, followed by the right and noncoronary leaflets, and rarely, the left and noncoronary leaflets (Supplemental Figures 1A, 1B).[1,22] The rarity of the third variant may relate to the varied rotational position of the aortic root, and the corresponding variability in the underlying myocardial vs fibrous support.[11,12]

When preparing for surgical repair, note should be taken of the height of the interleaflet triangles, which can accurately be measured using 3-dimensional imaging with multiplanar reformatting.[4,25] The leaflets themselves can be thickened, calcified, or fenestrated, as well as being compromised by subcommissural fusion. Should any components of the root be hypoplastic, this should be described (Supplemental Table 3).[4]

Bileaflet and bisinuate aortic valve

A minority of malformed roots, less than one-tenth, are built on a bisinuate scaffold.[23] These phenotypes are more frequent in

https://doi.org/10.1017/S1047951123001233 Published online by Cambridge University Press

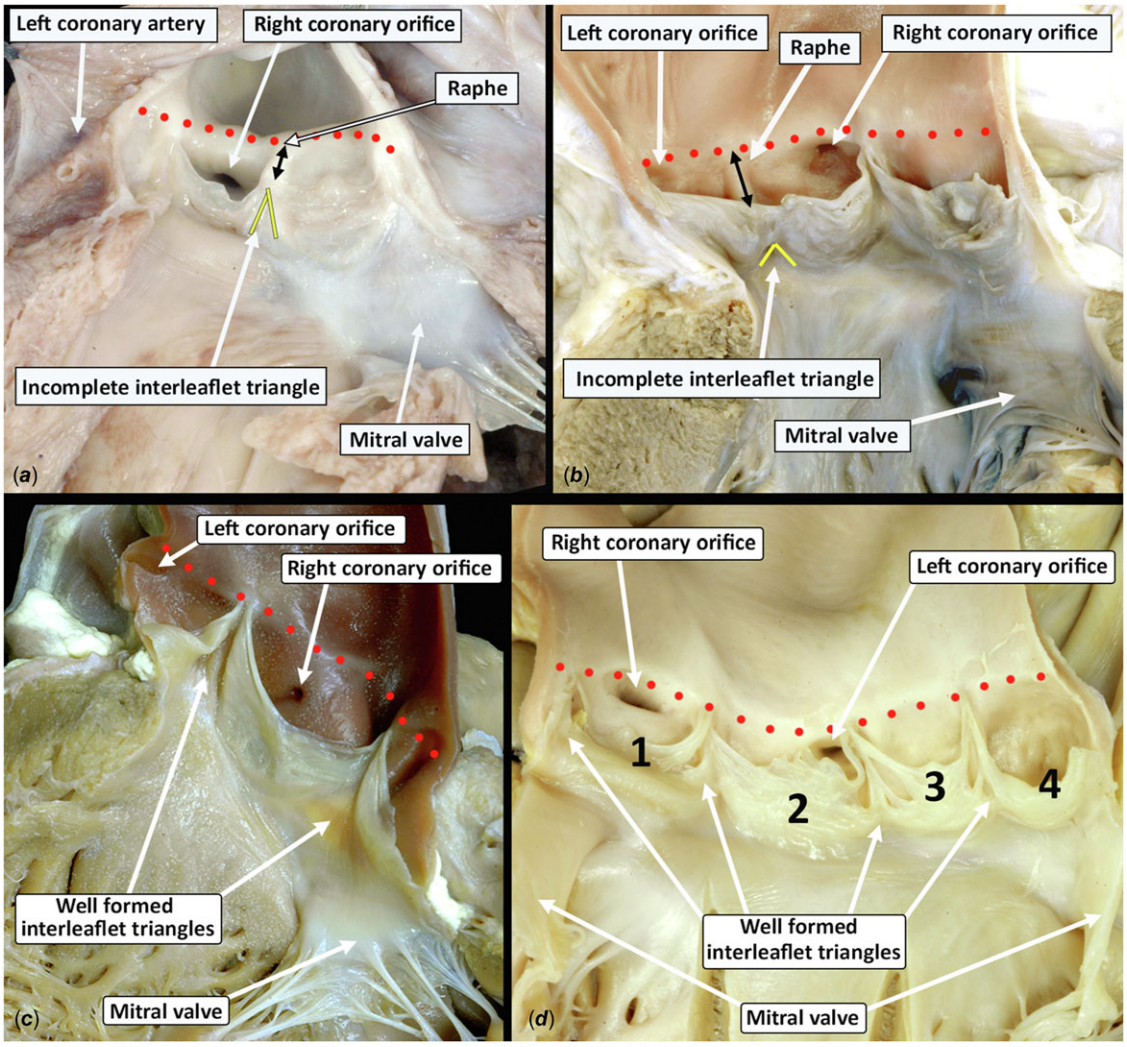

Figure 4. (A, B) Two different functionally bileaflet aortic valves. (A) Partial fusion between the right and noncoronary leaflets, with the zone of fusion (black double-headed arrow) representing <50% of the zone of apposition. (B) A functionally bileaflet aortic valve with greater fusion between the coronary leaflets and lower height of the corresponding interleaflet triangle (yellow caret). This reduces the aortic valvar opening area and tilts its plane at a greater angle relative to that of the sinutubular junction. (C) The bileaflet aortic valve with bisinuate aortic root. There are 2 leaflets, sinuses, and normal size interleaflet triangles, both with their apex reaching to the plane of the sinutubular junction (red dotted line). (D) A quadrileaflet and quadrisinuate aortic root, also without fusion between any of the leaflets, and therefore functioning as a quadrileaflet valve.

syndromes, particularly in Turner syndrome, which has the highest penetrance of bicuspid aortic valves, regardless of the valvar phenotype.[26] The root with 2 leaflets and 2 sinuses has only 2 interleaflet triangles, each of normal height, and hence equating to 2 normal commissures (Figure 4C). The normal height of the interleaflet triangles provides an orifice relatively parallel to the normal plane of the sinutubular junction.[6] This feature probably accounts for the lower propensity for ascending aortic dilation when compared with the functionally bileaflet variant. The paired leaflets and sinuses can be positioned anteroposteriorly or laterolaterally (Supplemental Figures 1C, 1D). The leaflets can be additionally malformed, be associated with subvalvar lesions impacting on leaflet motion, or the root itself can be hypoplastic.[4]

Functionally unileaflet aortic valve

The functionally unileaflet, or "unicuspid," variant is built on a trisinuate scaffold. Considered rare in the adult populations,[27,28] its true prevalence is likely underestimated due to misdiagnosis as a functionally bileaflet valve.[28,29] In newborns, it is the commonest form of critical aortic stenosis.[6] Its leaflets show 2 zones of fusion, each with a corresponding raphe and hypoplasia of the corresponding interleaflet triangle. Most commonly, the solitary zone of apposition is between the noncoronary and left coronary leaflets, with the solitary commissure positioned above the aortic-mitral curtain (Figure 5; Supplemental Video 1).[6] The lines of attachment of the conjoined leaflets are much closer to being truly annular.[30] When found in neonates or infants, the leaflets tend to be severely thickened (Figures 5A, 5B), but in adolescents or adults, there tends to be less complete fusion between the leaflets, with a greater opening area, and a less annular line of leaflet attachment (Figures 5C, 5D; Supplemental Figure 3).[6] Either way, the 3-dimensional plane of the aortic valvar opening area is at a significantly increased angle relative to the long axis of the ascending aorta compared with the functionally bileaflet form (Supplemental Figure 3C; Supplemental Video 2).[4] This results in an increased perturbance of flow.[31]

In this light, it becomes intuitive that studies support early progression toward valvar dysfunction and dilation of the thoracic aorta in those with a functionally unileaflet aortic valve.[32] These

https://doi.org/10.1017/S1047951123001233 Published online by Cambridge University Press

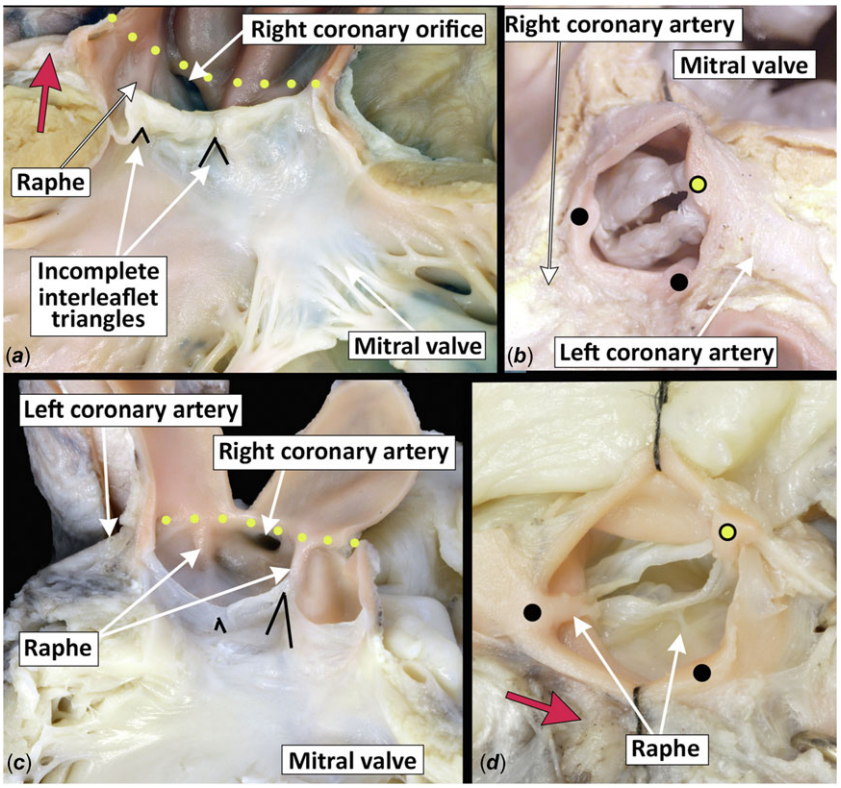

Figure 5. Two functionally unileaflet and trisinuate aortic roots are shown with fusion between the right and left, and right and noncoronary leaflets (black dots mark the zones of fusion, and the yellow dot with the black border marks the normal commissure). (A, B) A greater degree of fusion is seen in this heart between both pairs of leaflets, with smaller interleaflet triangles. (C, D) The corresponding interleaflet triangles in this heart are larger. (A, B) Much thicker aortic valvar leaflets are additionally demonstrated. This combination results in a much smaller aortic valvar opening area. The difference in interleaflet triangle heights dictates the degree of inferior tilting of the aortic valvar opening area of the involved adjacent leaflets. (A, D) The red arrows mark the left coronary artery. The yellow dotted line represents the sinutubular junction.

theories, however, require further investigation. Misdiagnosis may relate to the through-plane motion of 2-dimensional echocardiography, which can suggest that the zone of apposition has been interrogated in its entirety.[33] To avoid this problem, it is advantageous also to use 3-dimensional echocardiography (Supplemental Video 3).[25] If being considered for surgical repair, all features should all be interrogated by 3-dimensional imaging with multiplanar reformatting.[4,25] The leaflets themselves are usually abnormal, particularly when encountered in neonates, and are usually associated with hypoplasia of the aortic root.[4]

Quadrileaflet aortic valve and its functional counterparts

The quadrileaflet, or "quadricuspid," variant is extremely rare,[34] accounting for 0.005% of adults undergoing cardiac imaging.[35] The quadrisinuate root, without fusion between the leaflets, functions as the name suggests (Figure 4D). Fusion, nonetheless, can produce functionally trileaflet, bileaflet, and unileaflet variants. The functionally trileaflet valve within a quadrisinuate root, however, is markedly different from the normal trileaflet and trisinuate root. There can be marked asymmetry between the leaflets and sinuses. The coronary arteries most often arise from adjacent aortic sinuses, although they can arise from opposite aortic sinuses.[34] The wide variation does not lend itself to alpha-numeric classification. Description is the better approach. The variability in location of the coronary arteries defeats any description of "coronary aortic sinuses."[34] Three-dimensional imaging provides the information needed for surgical repair.[4,25] As with the other phenotypes, description should additionally include the leaflet substrate, any subvalvar substrate impacting leaflet motion, and whether the aortic root is hypoplastic.[4] This descriptive approach can also be applied to the variable truncal valvar morphologies seen in those born with a common arterial trunk.

Additional congenital and acquired abnormalities

Attention should be directed in all variants toward the presence of thickening or nodularity, perforation,[36] fenestration,[37] elongation, retraction, bending,[38] prolapse, flail, or billowing of the leaflets. A leaflet may rarely be absent[30] or duplicated (Supplemental Table 3). If present, the location of the associated calcification should be described. Calcification along a zone of apposition can produce acquired fusion, thus mimicking congenital fusion.[39,40] Dilation can involve any part of the root or the ascending aorta. Abnormal function can reflect obstruction to flow, with stenosis within the left ventricular outflow tract or at the level of the leaflets or sinutubular junction, or incompetency of the valve.

Mention is required of the aortoventricular tunnel. This channel bypasses the attachment line of a leaflet, producing a passage from the valvar sinus into the left or right ventricle. This can be accompanied by bileaflet, dysplastic, or ectopic aortic valvar tissue.[41] Abnormal communications can also result from rupture of an acquired or congenital aneurysm of a sinus of Valsalva, infective endocarditis, aortic dissection, and traumatic or iatrogenic injury.

Two-dimensional assessment of the normal and congenitally malformed aortic root

Normal aortic root dimensions

Accurate imaging requires an adequate terminology. The virtual basal ring extends between the nadirs of the semilunar leaflets. Long-axis 2-dimensional imaging will hover between an off-center plane joining the nadirs of the right and noncoronary leaflets and a nonspecific center plane.[42,43] It is difficult to be sure of the true plane of the virtual basal ring itself without the use of 3-dimensional imaging and multiplanar reformatting.[4] Long-axis imaging,

https://doi.org/10.1017/S1047951123001233 Published online by Cambridge University Press

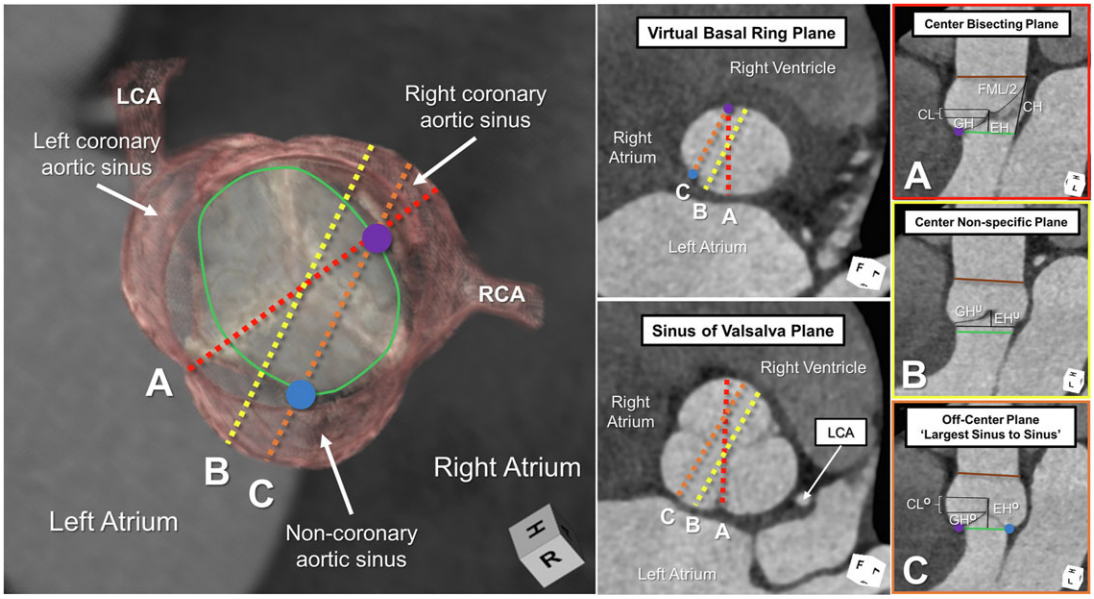

Figure 6. The left-side image demonstrates a 3-dimensional reconstruction of a normal aortic root in diastole, with the virtual basal ring marked with the green oval. The blue and purple circles mark the nadirs of the assessed leaflets. The middle panels demonstrate short-axis 2-dimensional planes at the virtual basal ring and aortic root. (A-C) The right-side panels are framed in the color of the corresponding colored dashed lines in the left-side panels. Only the center bisecting plane (A), with accurate marking of the virtual basal ring plane using multiplanar reformatting, permits precise measurement of the effective height (EH), coaptation length (CL), geometric height (GH), commissural height (CH), and free margin length (FML). Long-axis imaging of the aortic root, as obtained by 2-dimensional echocardiography, hovers between lines B and C, leading to underestimation (superscript U) and overestimation (superscript O) of these various metrics. The brown line represents the plane of the sinutubular junction. (LCA, left coronary artery; RCA, right coronary artery.)

in the absence of such 3-dimensional imaging, often cuts the virtual basal ring in oblique fashion, with an increasing value achieved when moving toward a nonspecific center plane (Figure 6).[44] These caveats underscore the limitations of the continuity equation in assessing the dimensions of the oval virtual basal ring.

Two-dimensional assessment of the sinuses by long-axis imaging provides a maximal dimension when moving from the off-center plane joining the nadirs of the visualized leaflets toward a nonspecific center plane. An apparent decrease in the coaptation length will be noted centrally (compare Figure 2 and Figure 6). This provides a clue that the cut plane is approaching the central zone of coaptation.[4,8,43]

Three separate methods have been proposed to measure the short axis of the root (Supplemental Figure 4). Of these measurements, 2 carry the name "cusp-to-cusp." The original method is better described as "largest sinus-to-sinus" dimension. The more recent method provides a "center of sinus-to-center of sinus" measurement,[44] which correlates well with long-axis measurements.[45] Only the "largest sinus-to-sinus" dimensions have normative values established in adults using magnetic resonance imaging.[46] The "cusp-to-commissure" method, more accurately described as "center of sinus-to-opposite commissure," does have normative adult values.[44] This method correlates strongly with 3-dimensional volumes.[7] No evidence currently supports the use of one method over the others, nor are we aware of any evidence to suggest the benefits of measuring "leading edge to leading edge" vs "inner edge to inner edge," or using a specific time of the cardiac cycle. Institutional consistency is therefore paramount, with reporting provided of both the method used and the timing of the cardiac cycle.

Compared with the virtual basal ring, the sinutubular junction is relatively more circular. Its plane differs by approximately 5° to 10° relative to that of the virtual basal ring, with a lower tilt angle produced during ventricular systole.[6,17]

Dimensions of the congenitally malformed aortic root

Assessing dimensions becomes increasingly complex when the root is congenitally malformed. In the functionally unileaflet and bileaflet roots, there is frequent significant asymmetry between the aortic leaflets and sinuses, potentially making transthoracic echocardiography inaccurate in this setting.[47] This technique should maintain its central role in the serial follow-up, but there should be a lower threshold also for obtaining cross-sectional imaging to provide the most accurate measurements. The cross-sectional methods established for the trisinuate root are inappropriate for measuring the bisinuate root. Instead, it may be more appropriate to measure from center of sinus-to-center of sinus, with subsequent measurement from commissure-to-commissure.[44] Similarly, trisinuate methods should not be applied to the quadrisinuate root. All said, there are no normative values for comparison to these patients without a trisinuate root. In the congenitally malformed aortic root with hypoplasia of 1 or more interleaflet triangles, furthermore, it becomes challenging to define the plane of the sinutubular junction. In these rare variants, suggested methods thus far are guided by opinion only. When monitoring these patients, given the complexity of measuring the congenitally malformed aortic root, it may be helpful to measure cross-sectional areas or three-dimensional volumes.[7]

Standardized assessment of aortic valvar dysfunction

Echocardiographic assessment of the degree of aortic valvar stenosis and regurgitation is well established, occasionally complimented by cardiac magnetic resonance imaging.[48] More recently, standard assessment of the aortic leaflets and their diastolic competency has been established using 3-dimensional imaging with multiplanar reformatting (Supplemental Table 1).[4,17,25] Such measurements have been used to guide a geometric approach toward surgical repair or preservation of the aortic valve.[49,50] They

https://doi.org/10.1017/S1047951123001233 Published online by Cambridge University Press

are commonly assessed in middiastole.[17,25,42] Accurate assessment, where a difference of a few millimeters becomes important, can only be achieved when using the center bisecting plane (Figure 6A, red dotted in the left-side panel), having accurately identified the plane of the virtual basal ring.[17,42]

The dimensions of the leaflets are based on their geometric height,[42,49,51] a curvilinear measurement taken within the extent of the root along the midline of the leaflet from its nadir at the virtual basal ring to the center point of its free margin edge, along with the free margin length, a curvilinear measure of the distance between the commissures along the edge of the leaflet.[42] The commissural height is the distance from the virtual basal ring along the long axis of an interleaflet triangle to the sinutubular junction. Comparison of these measurements becomes increasingly important in the congenitally malformed aortic root with 1 or more zones of fusion between the leaflets and with hypoplasia of the corresponding interleaflet triangles.

The coaptation length represents the linear extent of the segment of apposition involved at the central point of coaptation. When moving laterally from the center bisecting plane, the visualized coaptation length increases relative to the normal increased coaptation surface area along the lateral aspects of the zone of apposition (compare Figure 2 with Figure 6).[4,8] Standardized assessments, obtained from the central bisecting plane, are obtained at the central point of coaptation.[4] The effective height is the linear measurement from the center of the virtual basal ring to the cephalad edge of the central segment of coaptation of the leaflets. Normative values have now been reported intraoperatively,[8,51] and more recently for adults using computed tomography.[4]

Comment

After extensive discussions between members of the International Society for Nomenclature of Paediatric and Congenital Heart Disease, and other included experts relative to the assessment and management of the congenitally malformed aortic root, we offer here our suggestions for description of the congenitally malformed aortic root relative to the normal aortic root. The Nomenclature Society, constituted in 2005, produced the International Paediatric and Congenital Cardiac Code, which contains thousands of terms, each labeled with a 6-digit code. A "short list" of more than 350 items from this overall code has now been incorporated into the recently released 11th iteration of the International Classification of Diseases provided by the World Health Organization.[52] Our chosen terminologies of the aortic root are also consistent with those included in the most recent edition of the Terminologia Anatomica.[53] We anticipate that the content of this review will serve further to amend both the existing International Code and the congenital heart section of the International Classification of Diseases 11th Revision. They will hopefully serve as the basis for ongoing and future clinical care and research across all cardiac specialties.

Supplementary material. For supplementary material accompanying this paper visit https://doi.org/10.1017/S1047951123001233

Funding source. The authors have no funding sources to disclose.

Disclosure. The authors have no conflicts of interest to disclose.

References

1. Sievers HH, Schmidtke C. A classification system for the bicuspid aortic valve from 304 surgical specimens. J Thorac Cardiovasc Surg. 2007;133:1226–1233.
2. Michelena HI, Della Corte A, Evangelista A, et al. Speaking a common language: introduction to a standard terminology for the bicuspid aortic valve and its aortopathy. Prog Cardiovasc Dis. 2020;63:419–424.
3. Michelena HI, Della Corte A, Evangelista A, et al. International consensus statement on nomenclature and classification of the congenital bicuspid aortic valve and its aortopathy, for clinical, surgical, interventional and research purposes. Ann Thorac Surg. 2021;112:e203–e235.
4. Tretter JT, Izawa Y, Spicer DE, et al. Understanding the aortic root using computed tomographic assessment—a potential pathway to improved customized surgical repair. Circ Cardiovasc Imaging. 2021;14:e013134.
5. Anderson RH. Clinical anatomy of the aortic root. Heart. 2000;84:670–673.
6. Tretter JT, Spicer DE, Mori S, Chikkabyrappa S, Redington AN, Anderson RH. The significance of the interleaflet triangles in determining the morphology of congenitally abnormal aortic valves: implications for noninvasive imaging and surgical management. J Am Soc Echocardiogr. 2016;29:1131–1143.
7. Suzuki M, Mori S, Izawa Y, et al. Three-dimensional volumetric measurement of the aortic root compared to standard two-dimensional measurements using cardiac computed tomography. Clin Anat. 2021;34:333–341.
8. De Kerchove L, Momeni M, Aphram G, et al. Free margin length and coaptation surface area in normal tricuspid aortic valve: an anatomical study. Eur J Cardiothorac Surg. 2018;53:1040–1048.
9. Tretter JT, Spicer DE, Jacobs JP, Anderson RH. The aortic valve with two leaflets. JTCVS Open. 2021;9:89–90.
10. Toh H, Mori S, Tretter JT, et al. Living anatomy of the ventricular myocardial crescents supporting the coronary aortic sinuses. Semin Thorac Cardiovasc Surg. 2020;32:230–241.
11. Tretter JT, Mori S, Saremi F, et al. Variations in rotation of the aortic root and membranous septum with implications for transcatheter valve implantation. Heart. 2018;104:999–1005.
12. Amofa D, Mori S, Toh H, et al. The rotational position of the aortic root related to its underlying ventricular support. Clin Anat. 2019;32:1107–1117.
13. Sievers HH, Hemmer W, Beyersdorf F, et al. The everyday used nomenclature of the aortic root components: the tower of Babel? Eur J Cardiothorac Surg. 2012;41:478–482.
14. Anderson RH, Spicer DE, Quintessenza JA, Najm HK, Tretter JT. Words and how we use them—which is to be the master? J Card Surg. 2022;37:2481–2485.
15. Sutton JP 3rd, Ho SY, Anderson RH. The forgotten interleaflet triangles: a review of the surgical anatomy of the aortic valve. Ann Thorac Surg. 1995;59:419–427.
16. de Kerchove L, Boodhwani M, Glineur D, Noirhomme P, El Khoury G. A new simple and objective method for graft sizing in valve-sparing root replacement using the reimplantation technique. Ann Thorac Surg. 2011;92:749–751.
17. Izawa Y, Mori S, Tretter JT, et al. Normative aortic valvar measurements in adults using cardiac computed tomography-a potential guide to further sophisticate aortic valve-sparing surgery. Circ J. 2021;85:1059–1067.
18. Mori S, Tretter JT, Toba T, et al. Relationship between the membranous septum and the virtual basal ring of the aortic root in candidates for transcatheter implantation of the aortic valve. Clin Anat. 2018;31:525–534.
19. Tawara S. Das Reizleitungssystem des Säugetierherzens. Gustav Fischer; 1906.
20. Zimmerman J, Bailey CP. The surgical significance of the fibrous skeleton of the heart. J Thorac Cardiovasc Surg. 1962;44:701–712.
21. Macías Y, Tretter JT, Sánchez-Quintana D, et al. The atrioventricular conduction axis and the aortic root—inferences for transcatheter replacement of the aortic valve. Clin Anat. 2022;35:143–154.
22. Sabet HY, Edwards WD, Tazelaar HD, Daly RC. Congenitally bicuspid aortic valves: a surgical pathology study of 542 cases (1991 through 1996) and a literature review of 2,715 additional cases. *Mayo Clin Proc.* 1999;74:14-26.

23. Sillesen AS, Vøgg O, Pihl C, et al. Prevalence of bicuspid aortic valve and associated aortopathy in newborns in Copenhagen, Denmark. JAMA. 2021;325:561–567.
24. de Kerchove L, Mastrobuoni S, Froede L, et al. Variability of repairable bicuspid aortic valve phenotypes: towards an anatomical and repair-oriented classification. Eur J Cardiothorac Surg. 2019;ezz033.
25. Hagendorff A, Evangelista A, Fehske W, Schäfers HJ. Improvement in the assessment of aortic valve and aortic aneurysm repair by 3-dimensional echocardiography. JACC Cardiovasc Imaging. 2019;12:2225–2244.
26. Klásková E, Zapletalová J, Kaprálová S, et al. Increased prevalence of bicuspid aortic valve in Turner syndrome links with karyotype: the crucial importance of detailed cardiovascular screening. J Pediatr Endocrinol Metab. 2017;30:319–325.
27. Novaro GM, Mishra M, Griffin BP. Incidence and echocardiographic features of congenital unicuspid aortic valve in an adult population. J Heart Valve Dis. 2003;12:674–678.
28. Roberts WC, Ko JM. Frequency by decades of unicuspid, bicuspid, and tricuspid aortic valves in adults having isolated aortic valve replacement for aortic stenosis, with or without associated aortic regurgitation. Circulation. 2005;111:920–925.
29. Slostad BD, Witt CM, O'Leary PW, et al. Unicuspid aortic valve: demographics, comorbidities, echocardiographic features, and long-term outcomes. Circulation. 2019;140:1853–1855.
30. Tretter JT, Steffensen T, Westover T, Anderson RH, Spicer DE. Developmental considerations with regard to so-called absence of the leaflets of the arterial valves. Cardiol Young. 2017;27:302–311.
31. Entezari P, Schnell S, Mahadevia R, et al. From unicuspid to quadricuspid: influence of aortic valve morphology on aortic three-dimensional hemodynamics. J Magn Reson Imaging. 2014;40:1342–1346.
32. Mookadam F, Thota VR, Garcia-Lopez AM, et al. Unicuspid aortic valve in adults: a systematic review. J Heart Valve Dis. 2010;19:79–85.
33. Ewen S, Karliova I, Weber P, et al. Echocardiographic criteria to detect unicuspid aortic valve morphology. Eur Heart J Cardiovasc Imaging. 2019;20:40–44.
34. Tretter JT, Mori S, Spicer DE, Anderson RH. The aortic valve with four leaflets: how should we best describe this blue moon? Eur Heart J Cardiovasc Imaging. 2021;22:777–780.
35. Manuel AM, Ladeiras-Lopes R, Ribeiro J, et al. Prevalence, multimodality imaging characterization, and mid-term prognosis of quadricuspid aortic valves: an analysis of eight cases, based on 160,004 exams performed during 12 years in a tertiary care hospital. Eur Heart J Cardiovasc Imaging. 2021;22:765–776.
36. Hill AC, Bansal RC, Razzouk AJ, Liu M, Bailey LL, Gundry SR. Echocardiographic recognition of iatrogenic aortic valve leaflet perforation. Ann Thorac Surg. 1997;64:684–689.
37. Reade CC, Szeto WY, Bavaria JE. Aortic valve commissural fenestrations due to sinus of Valsalva dilatation. Ann Thorac Surg. 2009;87:646.
38. Soga F, Takaya T, Mori S, Nishii T, Hirata K. Bending of the aortic valvar leaflet causing severe aortic regurgitation in a patient with osteogenesis imperfecta. Eur Heart J Cardiovasc Imaging. 2016;17:708.
39. Pawade T, Sheth T, Guzzetti E, Dweck MR, Clavel MA. Why and how to measure aortic valve calcification in patients with aortic stenosis. JACC Cardiovasc Imaging. 2019;12:1835–1848.
40. Jilaihawi H, Makkar RR, Kashif M, et al. A revised methodology for aortic-valvar complex calcium quantification for transcatheter aortic valve implantation. Eur Heart J Cardiovasc Imaging. 2014;15:1324–1332.
41. McKay R, Anderson RH, Cook AC. The aorto-ventricular tunnels. Cardiol Young. 2002;12:563–580.
42. Mori S, Izawa Y, Shimoyama S, Tretter JT. Three-dimensional understanding of complexity of the aortic root anatomy as the basis of routine two-dimensional echocardiographic measurements. Circ J. 2019;83:2320–2323.
43. Mori S, Anderson RH, Tahara N, et al. The differences between bisecting and off-center cuts of the aortic root: the three-dimensional anatomy of the aortic root reconstructed from the living heart. Echocardiography. 2017;34:453–461.
44. Tretter JT, Mori S. Two-dimensional imaging of a complex three-dimensional structure: measurements of aortic root dimensions. J Am Soc Echocardiogr. 2019;32:792–794.
45. Rodríguez-Palomares JF, Teixidó-Tura G, Galuppo V, et al. Multimodality assessment of ascending aortic diameters: comparison of different measurement methods. J Am Soc Echocardiogr. 2016;29:819-826.e4.
46. Burman ED, Keegan J, Kilner PJ. Aortic root measurement by cardiovascular magnetic resonance: specification of planes and lines of measurement and corresponding normal values. Circ Cardiovasc Imaging. 2008;1:104–113.
47. Vis JC, Rodríguez-Palomares JF, Teixidó-Tura G, et al. Implications of asymmetry and valvular morphotype on echocardiographic measurements of the aortic root in bicuspid aortic valve. J Am Soc Echocardiogr. 2019;32:105–112.
48. Baumgartner H, Hung J, Bermejo J, et al. Recommendations on the echocardiographic assessment of aortic valve stenosis: a focused update from the European Association of Cardiovascular Imaging and the American Society of Echocardiography. J Am Soc Echocardiogr. 2017;30:372–392.
49. Schäfers HJ, Bierbach B, Aicher D. A new approach to the assessment of aortic cusp geometry. J Thorac Cardiovasc Surg. 2006;132:436–438.
50. Schäfers HJ. The 10 commandments for aortic valve repair. Innovations (Phila). 2019;14:188–198.
51. Schäfers HJ, Schmied W, Marom G, Aicher D. Cusp height in aortic valves. J Thorac Cardiovasc Surg. 2013;146:269–274.
52. Jacobs JP, Franklin RCG, Béland MJ, et al. Nomenclature for pediatric and congenital cardiac care: unification of clinical and administrative nomenclature—the 2021 International Paediatric and Congenital Cardiac Code (IPCCC) and the Eleventh Revision of the International Classification of Diseases (ICD-11). Cardiol Young. 2021;31:1057–1188.
53. International Federation of Associations of Anatomists. Federative International Programme for Anatomical Terminology (FIPAT). Terminologia Anatomica. 2nd ed, 2020. Accessed January 12, 2023. https://fipat.library.dal.ca/TA2/

https://doi.org/10.1017/S1047951123001233 Published online by Cambridge University Press